molecular pharmaceutics

pubs.acs.org/molecularpharmaceutics

Article

Old Dog New Tricks: PLGA Microparticles as an Adjuvant for Insulin Peptide Fragment-Induced Immune Tolerance against Type 1 Diabetes

Mohan Liu, Dandan Feng, Xiaoyu Liang, Min Li, Jing Yang, Hai Wang, Liyun Pang, Zhimin Zhou, Zhimou Yang, Deling Kong, and Chen Li*

Cite This: *Mol. Pharmaceutics* 2020, 17, 3513−3525

Read Online

ACCESS | Metrics & More | Article Recommendations | Supporting Information

ABSTRACT: Poly[lactic-*co*-(glycolic acid)] (PLGA) is arguably one of the most versatile synthetic copolymers used for biomedical applications. In vivo delivery of multiple substances including cells, pharmaceutical compounds, and antigens has been achieved by using PLGA-based micro-/nanoparticles although, presently, the exact biological impact of PLGA particles on the immune system remains controversial. Type 1 diabetes (T1D) is one subtype of diabetes characterized by the attack of immune cells against self-insulin-producing pancreatic islet cells. Considering the autoimmune etiology of T1D and the recent use of PLGA particles for eliciting desired immune responses in various aspects of immunotherapy, for the present study, a combination of $Ins2_{9-23}$ peptide (a known autoantigen of T1D) and PLGA microparticles was selected for T1D prevention assessment in nonobese diabetic (NOD) mice, a well-known animal model with spontaneous development of T1D. Thus, inoculation of PLGA microparticles + $Ins2_{9-23}$ completely prevented T1D development, significantly better than untreated controls and mice treated by either PLGA microparticles or $Ins2_{9-23}$ per se. Subsequent mechanistic investigation further revealed a facilitative role of PLGA microparticles in immune tolerance induction. In summary, our data demonstrate an adjuvant potential of PLGA microparticles in tolerance induction and immune remodulation for effective prevention of autoimmune diseases such as T1D.

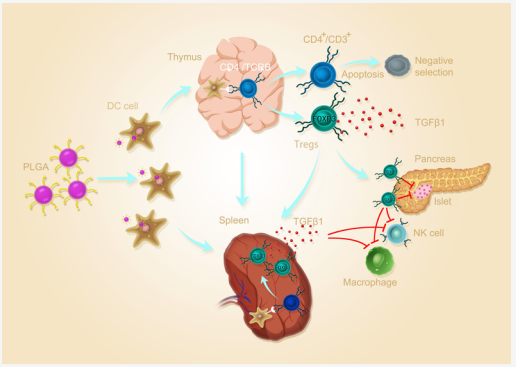

KEYWORDS: *type 1 diabetes, immune tolerance, PLGA microparticles, Treg, insulin*

1. INTRODUCTION

Diabetes is a chronic metabolic disorder, currently afflicting approximately 500 million people worldwide. In particular, the rates of type 1 diabetes (T1D, previously known as insulin-dependent juvenile or childhood-onset diabetes) in people under the age of 18 years have increased dramatically.[1,2] T1D is an autoimmune disorder characterized by autoreactive T-lymphocyte-mediated immune attack of insulin producing β-cells in the pancreatic islets. As islet β-cells are the only source of insulin in humans and mammals, the loss of β-cell function and/or β-cell destruction often means insufficient production of insulin. This leads to elevated blood glucose levels for a sustained period of time and, ultimately, the onset of diabetes.[1,3]

The exact mechanisms that are responsible for causing T1D are currently unknown, although both genetic and environmental factors are important in T1D progression.[4] Nowadays, the therapeutic option for T1D individuals is limited to insulin replacement therapy. However, despite the major advancement that has been achieved in terms of mimicking the endogenous insulin action with various insulin products, most T1D patients still fall short of meeting the required glycemic target.[5] The recent therapeutic development has been to target more specifically against autoreactive T lymphocytes that attack pancreatic β-cells,[3] for example, monoclonal antibodies against the T-cell CD3 receptor (commercial name: teplizumab and otelixizumab), CTLA4-immunoglobulin-mediated costimulatory inhibitor (abatacept), and fusion proteins that bind CD2 for targeting $CD4^+$ and $CD8^+$ effector memory T-cells (alefacept). However, aside from their less than satisfactory outcome in clinical trials,[6−8] these drugs are pan immunosuppressants that cannot distinguish autoantigen-attacking T-cells from other T-cells necessary for daily protection against environmental pathogens.

Received: May 14, 2020
Revised: July 29, 2020
Accepted: July 30, 2020
Published: July 30, 2020

https://dx.doi.org/10.1021/acs.molpharmaceut.0c00525
Mol. Pharmaceutics 2020, 17, 3513−3525

The concept of "vaccine" development has been proposed to induce tolerance against T1D. In fact, exposure to autoimmune disease-associated antigens has long been used to introduce immune tolerance in diseases such as multiple sclerosis,[9,10] allergy,[11] celiac disease,[10,12] and T1D.[13−15] This approach offers the possibility to "re-educate" the immune system to tolerate islet self-antigens (autoantigens) without the need for systemic immunosuppression. Several autoantibodies against islet autoantigens, such as insulin, islet cell autoantibodies (ICAs), glutamate decarboxylase protein (GAD65), and zinc transporter protein (ZnT8), have all been identified in T1D patients, although antigen-based trials that used different autoantigens have been less successful.[16,17]

Indeed, conventional strategies for effective vaccine development are dependent on the appropriate selection of antigens and presentation of antigen by immune cells for subsequent immunomodulatory impact, and the potency of a certain type of vaccine is often limited by the quantity of antigen that can be safely used for the inoculation and the antigen presentation process. However, both criteria can be benefited by the use of biomaterial-based antigen delivery systems, which would allow maximal antigen loading as well as sufficient antigen presentation. In recent years, the use of biomaterials for vaccine delivery has been extensively explored, and the potential to spatiotemporally regulate the activities of immune cells by employing biomaterial-based antigen delivery systems provides a promising platform to improve the efficacy and safety of conventional vaccines.[18−26] As recently been reviewed by Kwiatkowski et al.,[25] multiple nano-/microparticle-based therapies have been investigated for their impact in modulating immune systems. For example, for autoimmune diseases, thiol−polyethylene glycol-coated gold nanoparticles that simultaneously deliver a myelin peptide antigen MOG_{35-55} and a nontoxic mucosal ligand resulted in the promotion of regulatory T-cell (Treg) expansion and suppression of autoimmune encephalomyelitis.[27] Artificial antigen presentation was another approach, by engineering artificial antigen presenting cells[28] or using, for instance, iron oxide nanoparticles coated with an islet peptide,[29] to achieve desirable T-cell manipulation. However, of all delivery systems, poly[lactic-*co*-(glycolic acid)] (PLGA) nano-/microparticles were the most used and reported.[14,25,26,30]

PLGA is one of the most extensively investigated copolymers in the field of biomedical research because of its biocompatibility and biodegradability.[31,32] It is well known that PLGA particles can be easily fabricated using the prevalent emulsion-solvent evaporation method.[33,34] Furthermore, there have been reports showing that functionalized PLGA-based nano- and microparticles could induce cytotoxic T-cell responses to eliminate tumor cells.[19−21,23] On the other hand, other studies observed tolerogenic properties of PLGA particles when used in combination with biological drugs,[20,23,35] antigens, and/or immune adjuvants.[14,22,24,36−40] More relevantly, it has been long proposed that PLGA microparticles were more likely to be taken up in vivo[24,28,36,38,40] and that immune adjuvant potential of PLGA microparticles has also been implicated previously.[41]

As a result, for the purpose of the present study, we chose to use PLGA microparticles instead of nanoparticles. The peptide fragment sequence 9 to 23 of the insulin B chain ($Ins2_{9-23}$), a known autoantigen with potent immune reactivity for tolerance induction in T1D,[42,43] was then loaded and delivered in vivo via PLGA microparticles to examine the potential of PLGA microparticles + $Ins2_{9-23}$ in T1D prevention. We report here an immune adjuvant property of PLGA microparticles for successful induction of immune tolerance in NOD mice by activating immune-related mechanisms in the thymus and spleen (Scheme 1). Considering the reported biological safety of PLGA and the insulin peptide fragment $Ins2^{9-23}$, data reported in the present study may also have positive implications on therapeutic investigation against T1D in humans.

Scheme 1. Schematic Representation of Mechanisms Likely Activated by the PLGA microparticles + $Ins2_{9-23}$ for Immune Tolerance Induction[a]

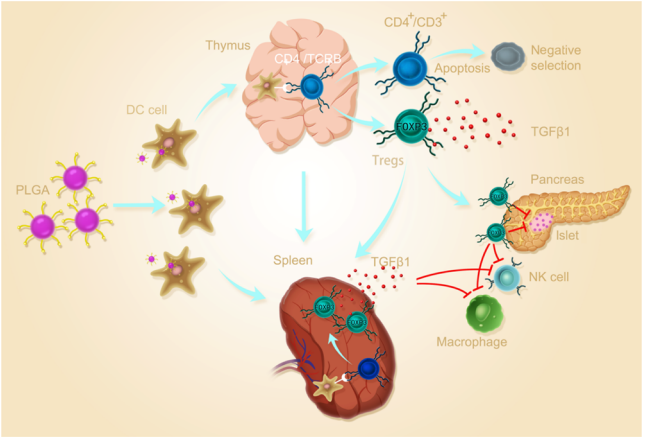

[a]PLGA microparticles may stimulate dendritic cell presentation of the autoantigen $Ins2_{9-23}$ via the MHC II pathway, which induces $CD4^+$/$TCR\beta^+$ differentiation in the thymus for negative selection or Treg generation. In the periphery, immune tolerance was also initiated via PLGA microparticle-dependent upregulation of splenic Treg population and TGF-β1 production. Both processes enable systemic immune tolerance of $Ins2_{9-23}$ and ameliorate immune cell infiltration in the pancreatic islets, which results in the prevention of T1D development.

2. EXPERIMENTAL SECTION

2.1. Materials. PLGA (M_w: ∼10k) and all cell culture reagents were purchased from Sigma-Aldrich (Shanghai, China). The $Ins2_{9-23}$ peptide (SHLVEALYLVCGERGR, M_w: 1.8 kDa, endotoxins < 1 EU mg^{-1}) and Cy5-$Ins2_{9-23}$ were supplied by Bankpeptide (Hefei, China). Antibodies used for flow cytometry analysis were from eBioscience (CA, USA) and antibodies used for immunofluorescence staining were from Abcam (Shanghai, China). Recombinant interleukin-4 (IL-4), interleukin-2 (IL-2), and granulocyte-macrophage colony-stimulating factor (GM-CSF) were from PeproTech (Rocky, Hill, USA). The antimouse CD11c magnetic beads were purchased from Miltenyi Biotec (Beijing, China), and the Detoxi-Gel Endotoxin Removing Gel was from Thermo Fisher Scientific (Beijing, China). Multiple cytokine enzyme-linked immunosorbent assay (ELISA) was performed by Luminex (Beijing, China). The MicroBCA protein assay kit was obtained from Thermo Fisher Scientific Inc. (Rockford, IL, USA) and the Tachypleus amebocyte lysate (TAL) was purchased from Xiamen Horseshoe Crab Reagent Manufactory Co., Ltd. Female NOD/ShiLtJNju mice were supplied by the Model Animal Research Center of Nanjing University. All animal procedures were approved by the Centre of Tianjin

https://dx.doi.org/10.1021/acs.molpharmaceut.0c00525
Mol. Pharmaceutics 2020, 17, 3513−3525

Animal Experiment Ethics Committee and authority for animal protection (approval no.: SYXK[Jin] 2011-0008).

2.2. Preparation and Characterization of PLGA Microparticles. Briefly, 150 mg of PLGA was first dissolved in 10 mL of dichloromethane to prepare the PLGA solution. Then, the PLGA solution was poured into a rapidly stirring PVA solution (100 mL, 1% [w/v]) at 8000 rpm for 5 min, and the mixture was maintained stirring at the same speed overnight at room temperature to allow the solvent to evaporate. To prepare $Ins2_{9-23}$-loaded PLGA microparticles, 40 mg of peptide was added to the PLGA solution (containing 100 mg of PLGA) and emulsified (80 W, 10 min, 30″−30″−30″−30″) in an ice bath before being added to the PVA solution. The resultant PLGA microparticles or $Ins2_{9-23}$-loaded PLGA microparticles were then centrifuged for 5 min at 7000 rpm, washed with deionized water three times, and freeze-dried for further use. The morphology of the PLGA microparticles was determined by scanning electron microscopy (SEM, ZEISS, SUPRA 55VP).

For loading capacity (LC), 2 mg of PLGA-$Ins2_{9-23}$ was dissolved in a final volume of 1 mL, and the value of LC was calculated as the percentage of weight of total protein minus unbound protein and divided by the total weight of microparticles. For encapsulation or loading efficiency (LE), as most peptides were thought to be adopted on the outer surface of PLGA microparticles, 10 mg of PLGA-$Ins2_{9-23}$ was used and dissolved in a final volume of 50 mL before ultraviolet (UV) absorbance measurements. LE was calculated as the percentage of weight of total protein minus weight of unbound protein divided by the total weight of protein.

2.3. In Vitro Peptide Release. The $Ins2_{9-23}$-loaded PLGA microparticles (circa 40 mg) were incubated at 37 °C in 10 mL incubation buffer [phosphate-buffered saline (PBS) containing 1% bovine serum albumin (BSA) and 1% penicillin/streptomycin, pH = 7.4] and kept in continuous agitation by an orbital shaker. Samples were taken at designated time points, followed by centrifugation at 12,000 rpm for 10 min (i.e., the volume removed during sampling was replaced with the same amount of incubation buffer), and stored at −80 °C. The content of peptide within each sample was quantified using the BCA protein assay, as previously detailed.[18]

2.4. In Vitro Antigen Presentation Assessment with Bone Marrow-Derived Dendritic Cells. Bone marrow-derived dendritic cells (BMDCs) were obtained from the hind limb bones of female NOD mice (8 weeks old), as reported previously,[18] and seeded in six-well plates at a density of 4×10^6 cells per well. BMDCs were then maintained in complete cell culture media (RPMI 1640 supplemented with 10% FBS, 100 U/mL penicillin, 100 μg/mL streptomycin, 20 ng/mL GM-CSF, and 10 ng/mL IL-4) and kept under cell culture conditions (37 °C, 95% O_2/5% CO_2). On day 3, the culture media were carefully removed and replaced, and on day 5 of culturing, BMDCs were exposed to PLGA microparticles + $Ins2_{9-23}$, blank PLGA microparticles, and $Ins2_{9-23}$ at a concentration of 10 μg/mL. On day 7, most semiadhesive cells have acquired typical dendritic cell (DC) morphology and were harvested for flow cytometry analysis.

Thus, $CD11c^+$ DCs were isolated by antimouse CD11c magnetic beads (Miltenyi Biotech) according to the manufacturer's instructions. Cells were then exposed to antimouse MHC II (clone: AF6-120.1), antimouse MHC I (H-2Kb) (clone AF6-88.5.5.3), antimouse CD80 (clone: 16-10A1), and antimouse CD86 antibodies at 1 μg per 2×10^6 cells for 30 min on ice, following which the cells were washed twice with cold PBS and analyzed using BD FACSCalibur (BD Biosciences, San Jose, CA, USA).

2.5. In VitroBMDC Uptake of $Ins2_{9-23}$. BMDCs (1×10^6 cells/mL) were isolated and seeded in confocal laser scanning microscopy (CLSM) discs at a density of 2×10^6 cells per disc. On day 5, BMDCs were cocultured with Cy5-labeled $Ins2_{9-23}$ in the absence or presence of PLGA microparticles and maintained under cell culture conditions (37 °C, 95% O_2/5% CO_2) for 2 and 6 h. For peptide uptake quantification, flow cytometry analysis was performed, and the mean fluorescence intensity (MFI) was measured as the estimation of $Ins2_{9-23}$ internalization. For confocal microscopy, cells were then washed with PBS and fixed with 3.7% paraformaldehyde for 10−15 min before staining with 488-Phalloidin for 30 min. Cell nuclei were stained with 4′,6-diamidino-2-phenylindole (DAPI), and the cellular uptake was examined under a confocal microscope (TCS SP5II, Leica, Ernst-Leitz-Strasse, Germany).

2.6. T1D Prevention Study. Female NOD mice (4 weeks) were immunized subcutaneously under the front left leg with PLGA microparticles + $Ins2_{9-23}$ (peptide: 100 μg), blank PLGA microparticles (approximate equivalence to PLGA used for $Ins2_{9-23}$ loading in the PLGA microparticles + $Ins2_{9-23}$ group), $Ins2_{9-23}$ (100 μg), and endotoxin-free PBS once a week for 5 weeks (from 4 week old to 8 week old) and maintained in specific pathogen-free facilities for 30 weeks (n = 20 per group). Random plasma glucose level and body weight were recorded weekly from week 10 with a OneTouch Ultra blood glucometer (Lifescan Inc., Milpitas, CA, USA). An animal was classified as diabetic if the random plasma glucose level exceeds 11.1 mmol/L for 2 consecutive weeks. The intraperitoneal glucose tolerance test (IPGTT) was performed in mice from all treatment groups at weeks 12 and 20. Serum was obtained from all mice at the age of week 30, and multiple cytokine ELISA assay was performed by Luminex according to the manufacturer's instruction.

2.7. Lymphocyte Purification from the Thymus and Spleen. NOD mice were sacrificed and submerged in 75% ethanol for several minutes before dissection under aseptic conditions. The thymus or spleen was grinded in a 70 μm BD cell strainer in a lymphocyte extract solution and the lymphocytes were isolated by gradient purification (centrifugation at 800g for 30 min). The red blood cell lysis buffer was added for 2 min before being washed with PBS. Cells were then exposed to antimouse CD3, antimouse CD4, antimouse CD8, and antimouse TCRβ antibodies for 30 min at 4 °C, following which they were washed, centrifuged (1800 rpm, 5 min), and stored for flow cytometry analysis. For Treg labeling, cells were first exposed to antimouse CD4 and antimouse CD25 antibodies. Then, the cells were treated with BD permeabilization buffer at 4 °C overnight, antimouse FOXP3 antibodies were added, and the cells were incubated for further 30 min and analyzed immediately by flow cytometry.

2.8. Peptide Recall T-Cell Proliferation Assay. At week 30, randomly selected NOD mice were sacrificed, from which splenic and thymic T-cells were isolated and labeled with 5 μmol/L 5,6-carboxyfluorescein acetate N-succinimidyl ester (CSFE). The CFSE-labeled T-cells were then seeded in a 24-well plate at a density of 2×10^6 cells/well. Recombinant mouse IL-2 was added (0.5 ng/mL) to all treatment groups with 10 μg of $Ins2_{9-23}$ and the cells were maintained in culture for 3 days. T-cell proliferation was then examined by flow

https://dx.doi.org/10.1021/acs.molpharmaceut.0c00525
Mol. Pharmaceutics 2020, 17, 3513−3525

cytometry, in which percentages of $CD4^+CFSE^{low}$ and $CD8^+CFSE^{low}$ cells were analyzed.

2.9. Histological and Immunofluorescence Staining. Histological staining and immunostaining were carried out following previous procedures.[44,45] The pancreas and spleen were extracted and paraffin-embedded before sectioned (5 μm width) onto microscopic slides. They were then used for hematoxylin−eosin (H&E) or immunofluorescence staining. For immunofluorescence staining, tissue sections were treated with primary antibodies at 4 °C overnight. The sections were then washed with PBS and stained with a secondary antibody for 1−2 h at room temperature and examined under a fluorescence microscope.

2.10. Detection of Endotoxin. The endotoxin levels of all samples were measured using a TAL chromogenic endpoint assay according to the manufacturer's instruction. Briefly, standards or samples were plated in designated wells (100 μL), followed by addition of TAL reagent. The mixture was then incubated at 37 °C for 1 h. A chromogenic substance was then added, followed by the azoic reagent for the colorimetric reaction. The optical density was then recorded for each well at 545 nm by a microplate reader (BioTek, USA). In order to minimize endotoxin contamination, all plastics were sterilized and glassware were roasted in an oven at 250 °C for 1 h. Regarding reagents that cannot be exposed to high temperatures, they were passed through the Detoxi-Gel Endotoxin Removing Gel for endotoxin removal.

2.11. Statistical Analysis. All data are presented as means ± standard error of means (s.e.m.). Statistical analysis was performed using GraphPad Prism Software (CA, USA). For multiple group comparison, one-way analysis of variance (ANOVA) analysis was employed with Tukey's post hoc test. Differences were considered statistically significant, if the P value was below 0.05.

3. RESULTS AND DISCUSSION

3.1. Characterization of PLGA Microparticles. Figure 1 shows the typical PLGA microparticles fabricated by the emulsion-solvent evaporation method, as we have reported previously.[33,46] Considering the reported potency and lack of metabolic activity of $Ins2_{9-23}$,[42,43] $Ins2_{9-23}$ was selected as autoantigen in this study and loaded onto the PLGA microparticles for tolerance induction against T1D. For both PLGA and peptide-loaded PLGA microparticles, a spherical particle shape was observed (Figure 1). The average particle size ranges between ∼1 and 2 μm in diameter for PLGA microparticles and ∼2−4 μm for $Ins2_{9-23}$-loaded PLGA microparticles, with PDI (polydispersity index) values of 0.292 ± 0.082 and 0.241 ± 0.044 for PLGA and $Ins2_{9-23}$ PLGA microparticles, respectively (Figure 1B and Table 1), corresponding to images obtained by SEM (Figure 1A). The LE and LC were also assessed as shown in Table 1, indicating sufficient antigen delivery capacity of PLGA microparticles.

The in vitro peptide-releasing profile (Figure 1C) demonstrates a rapid release of $Ins2_{9-23}$ by the PLGA microparticles. Indeed, by fitting the peptide release profiles to several release models (zero order, first order, Higuchi, Weibull, and Ritger−Peppas), we found that it is better fitted with both Weibull and Ritger−Peppas equations (Table 2). Regarding the Ritger−Peppas release model, the equation describes that for the Fickian diffusion process, the n value is 0.30 ± 0.01, and for the Case-II transport process, the n value equals 0.45 ± 0.02 for polydispersable particles. As a result, the in vitro release of

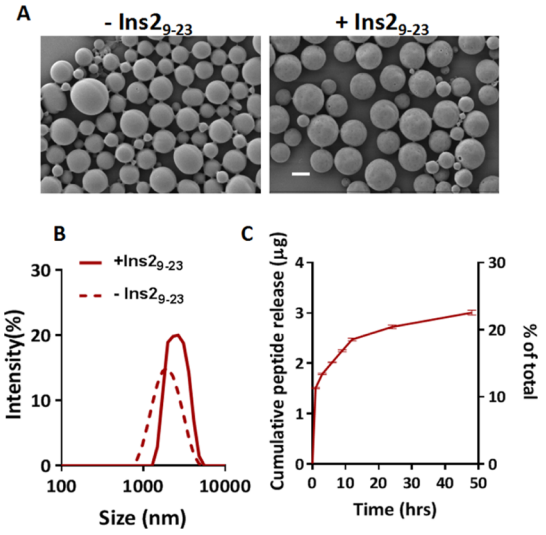

Figure 1. Characterization of PLGA microparticles. (A) Representative SEM images of blank PLGA microparticles and $Ins2_{9-23}$-loaded PLGA microparticles. Scale bar = 2 μm. (B) Size distribution of microparticles by dynamic light scattering. Red solid line: Ins29-23-loaded PLGA microparticles. Red dotted line: blank PLGA microparticles. (C) Cumulative in vitro $Ins2_{9-23}$ release by PLGA microparticles of different molecular weights. Data represent mean ± s.e.m, n = 3.

$Ins2_{9-23}$ by PLGA microparticles, with n = 0.238 ± 0.014, is thought to be primarily controlled by Fickian diffusion ($n \leq 0.31$).[34]

3.2. PLGA Microparticles Enhanced the DC uptake and Presentation of $Ins2_{9-23}$. To examine the cellular uptake ability of the $Ins2_{9-23}$ peptide in the presence and absence of PLGA microparticles, Cy5-labeled-$Ins2_{9-23}$ were loaded onto the PLGA microparticles and cocultured with BMDCs. We observed a sustained level of antigen uptake over a period of 6 h, following the coculturing of PLGA microparticles + $Ins2_{9-23}$ (PLGA[PEP]; Figure 2A,B). This is consistent with the rapid initial peptide-releasing kinetics we have observed for the PLGA microparticles (Figure 1C). Indeed, the antigen uptake capacity of BMDCs that were cocultured with PLGA(PEP) and of those cocultured with the $Ins2_{9-23}$ peptide alone were similar at 2 h (94 ± 4% of PLGA(PEP) over peptide only, P > 0.1). However, at 6 h, while the antigen uptake level remains relatively unchanged for the PLGA(PEP) group (104 ± 1% over the 2 h peptide-only group; 110 ± 1% over PLGA(PEP) at 2 h, P > 0.1), the fluorescent signal that corresponds to the cellular antigen uptake showed significant drop-off in BMDCs cultured with $Ins2_{9-23}$ alone (50 ± 18% over the 2 h peptide-only group, P < 0.05). Our observation is in line with previous reports showing enhanced cellular uptake of biological drugs or peptide antigens using PLGA microparticles as delivery vehicles.[19−22]

Regarding the impact of PLGA on BMDC maturation, so far, the reports have been conflicting. Allen et al. reported an inhibitory effect of PLGA, albeit without any antigens, on BMDC maturation, implicating a tolerogenic property of PLGA per se.[36] Similarly, multiple studies from Kishimoto's group reported the ability of PLGA nanoparticles to induce antigen-specific immune tolerance in B-cells,[47] or reduce undesirable protein-induced hypersensitivity by rapamycin-loaded PLGA nanoparticles.[22] On the other hand, we have previously observed the stimulation of PLGA on DC

https://dx.doi.org/10.1021/acs.molpharmaceut.0c00525
Mol. Pharmaceutics 2020, 17, 3513−3525

Table 1. Physical Characterization of PLGA and $Ins2_{9-23}$-Loaded Microparticles. Data Are Presented as Mean ± Standard Deviation (n = 3)

microparticles	size (μm)	PDI[a]	zeta potential (mV)	LE[b]	LC[c]
PLGA	1.6 ± 0.05	0.292 ± 0.082	−27.9		
PLGA-$Ins2_{9-23}$	3.67 ± 0.24	0.241 ± 0.044	−10.5	20.66 ± 3.66	9.86 ± 0.15

[a]PDI, polydispersity index. [b]LE = (total protein − unbound protein)/total protein × 100%. [c]LC = (total protein − unbound protein)/total weight of microparticles × 100%.

Table 2. Release Models of Peptide-Loaded PLGA Microparticles

	PLGA-$Ins2_{9-23}$		
zero order	$y = 12.271 + 0.263t$	$R^2 = 0.748$	
first order	$y = 20.352(1 - e^{-0.255t})$	$R^2 = 0.690$	
Higuchi	$y = 2.352t^{0.5} + 8.259$	$R^2 = 0.923$	
Weibull	$y = 100(1 - e^{(0.0001(t-0.324))})^{0.246}$	$R^2 = 0.982$	
Peppas	$y = 9.443t^n$	$R^2 = 0.981$	$n = 0.238 \pm 0.014$

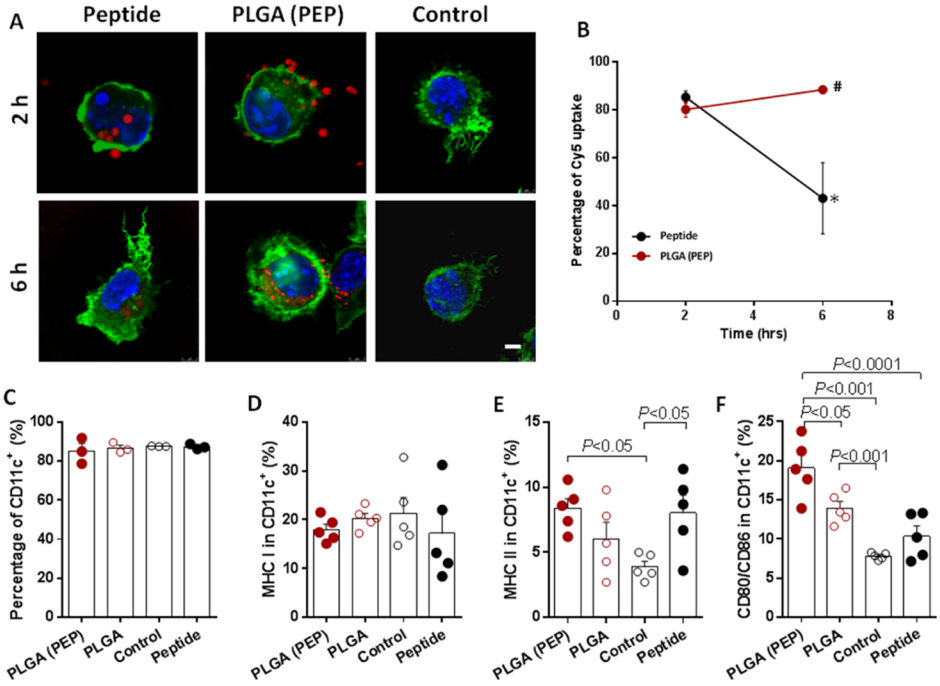

Figure 2. PLGA microparticles enhance in vitro antigen uptake and presentation in BMCDs. (A) Representative CLSM images of BMDCs that were cocultured with Cy5-labeled $Ins2_{9-23}$ and Cy5-$Ins2_{9-23}$-loaded PLGA microparticles for 2 and 6 h. Cells were stained with Phalloidin (green) and DAPI (blue). Scale bar = 2.5 μm. (B) MFI of Cy5 was quantified in BMDCs by flow cytometry. *$P < 0.05$ vs Peptide group at 2 h; #$P < 0.05$ vs Peptide group at 6 h. Statistical significance was assessed using Student's t-test. (C−F) Expression of DC surface markers following stimulation by $Ins2_{9-23}$ (Peptide), blank PLGA microparticles (PLGA), PLGA microparticles + $Ins2_{9-23}$ (PLGA[PEP]), and PBS (Control). Statistical significance was assessed using one-way ANOVA with Tukey's post hoc test. Data represent mean + s.e.m, n = 3−5.

maturation, though the PLGA nanoparticles were functionalized with hyaluronic acid in the formula.[48] PLGA−acetonitrile (PLGA−AC) nanoparticles were also demonstrated to increase the monocyte population when loaded with B16 melanoma tumor antigens.[21] Moreover, Verbeke et al. reported the proinflammatory property of the gel containing blank PLGA particles, partly shown as a higher level of IL-12p70, a secreted cytokine that was originally discovered for its ability to induce interferon-gamma (INF-γ) production and Th1 responses, although a systemic tolerance to T1D was ultimately reported.[37] In addition, PLGA microparticles were also reported to enhance antigen presentation and T-cell expansion in vitro,[49] all of which are implicative of a stimulatory role of PLGA particles on antigen presentation.

Thus, to determine the potential effect of PLGA microparticles during $Ins2_{9-23}$ delivery, we have isolated BMDCs from adult female NOD mice (8 weeks). The $CD11c^+$ DCs were pooled following magnetic bead selection (Figure 2C), and expression of antigen presentation cell markers, CD80/CD86, as well as of major histocompatibility complex class I (MHC I) and class II (MHC II), was examined by flow cytometry. We observed no significant differences in MHC I expression in $CD11c^+$ BMDCs (Figure 2D), which is expected of the conventional peptide antigen presentation pathway. This is because antigens presented via the MHC I molecule are often protein fragments from environmental bacteria and viruses, while antigens presented by the MHC II pathway are usually peptide taken up by DCs via endocytosis. Indeed, it has been reported that $Ins2_{9-23}$ binds to MHC II for subsequent

https://dx.doi.org/10.1021/acs.molpharmaceut.0c00525
Mol. Pharmaceutics 2020, 17, 3513−3525

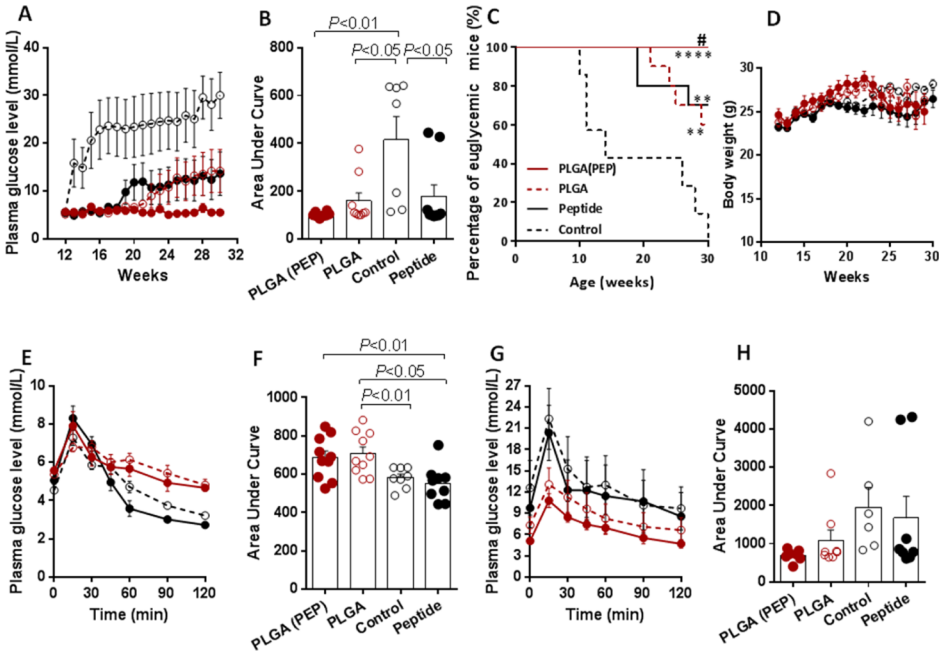

Figure 3. T1D prevention study. (A) Random plasma glucose concentrations of all mice up to the age of week 30. (B) Area under the curve (AUC) of the corresponding plasma glucose levels of mice of all four treatment groups. (C) Proportion of mice that achieved euglycemia following immunization with $Ins2_{9-23}$ (Peptide), blank PLGA microparticles (PLGA), PLGA microparticles + $Ins2_{9-23}$ (PLGA[PEP]), and PBS (Control). (D) Average body weight of all mice until the age of week 30. (E,G) Results of IPGTTs of all mice at the age of week 12 (E) and 20 (G). (F,H) AUC of the corresponding IPGTT values of all mice at the age of week 12 (F) and 20 (H). Data represent mean ± s.e.m, $n = 6-10$. Statistical significance was assessed using one-way ANOVA with Tukey's post hoc test. For the survival curve, statistical significance was assessed by log-rank Mantel−Cox and Gehan−Breslow−Wilcoxon tests. ****$P < 0.0001$, **$P < 0.01$ vs Control; $^{\#}P < 0.05$ vs PLGA group.

T-cell activation.[50] Moreover, as PLGA microparticles have been reported to facilitate the active endocytosis of monocytes, including DCs and macrophages, it is also likely to elicit the MHC II pathway.[24,28,36,38,40,41] The MHC I antigen presentation pathway is known as CD8 T-cell restricted (Th1) and antigens presented by MHC II would initiate CD4 helper T-cell (Th2) responses. Considering that the $Ins2_{9-23}$ peptide is part of the insulin B chain and, therefore, could be regarded as a self-antigen (or autoantigen), presentation of the $Ins2_{9-23}$ peptide would more likely involve the MHC II pathway. Indeed, we have detected an elevated level of MHC II expression in BMDCs that were exposed to $Ins2_{9-23}$ (Figure 2E; 207 ± 35% over Control, $P < 0.05$) as well as to PLGA microparticles + $Ins2_{9-23}$ peptide (Figure 2E; 216 ± 19% over control, $P < 0.05$). In addition, significant elevation of CD80/CD86 expression levels was observed from BMDCs of the PLGA microparticles + $Ins2_{9-23}$ peptide (PLGA[PEP]) group (Figure 2F). Interestingly, PLGA microparticles alone also enhanced the CD80/CD86 expression levels in BMDCs (Figure 2F; 178 ± 11% over Control, $P < 0.001$) but not MHC II as it lacks the peptide antigen $Ins2_{9-23}$. As BMDCs cocultured PLGA(PEP) showed increased levels of CD80/86 expression compared to BMDCs cocultured with $Ins2_{9-23}$ (Figure 2F, 184 ± 18% over the peptide group, $P < 0.0001$), both the above implicate a stimulatory impact of PLGA microparticles on DC antigen presentation.

3.3. PLGA Microparticles + $Ins2_{9-23}$ Immunization Prevented Immune Infiltration of Pancreatic Islets and the Onset of T1D in NOD Mice. Having confirmed that the PLGA microparticles enhanced the presentation of $Ins2_{9-23}$ via the MHC II pathway in DCs in vitro, we have subsequently tested whether the PLGA microparticles + $Ins2_{9-23}$ inoculation had any impact on diabetes progression in nonobese diabetic (NOD) mice. NOD mice are widely acknowledged as a type 1 diabetic model animal. In general, without intervention, the incidence of T1D onset occurs in 70−80% female NOD mice by the age of 30 weeks.[51] As for "immune re-education" with our PLGA microparticles + $Ins2_{9-23}$ "vaccine", female NOD mice were administered with low-dose $Ins2_{9-23}$ (with or without PLGA microparticles), from the age of 4 weeks for 5 consecutive weeks. Mice treated with blank PLGA microparticles and PBS were also included as parallel control groups.

Thus, random plasma glucose levels were recorded every week and, unsurprisingly, animals immunized with $Ins2_{9-23}$ showed 30% onset of T1D by week 30, similar to previous reports.[42,43] Notably, however, it was evident that mice inoculated with PLGA(PEP) remained euglycemic (plasma glucose level < 11.1 mmol/L) until the age of week 30 (Figure 3A−C; AUC: 25 ± 1% over Control, $P < 0.01$). Indeed, hyperglycemia was first detected in mice from the $Ins2_{9-23}$-only group at week 19 and for the PLGA-only group at week 21. However, for both groups, T1D progression still showed amelioration compared to the controls (AUC: 38 ± 8 and 43 ± 12% for PLGA and Peptide groups, respectively, % over Control, $P < 0.05$). As expected, the earliest onset of diabetes was detected in mice from the control group at week 10.

IPGTT was also performed in mice from all four groups at the age of weeks 12 and 20, and circulating insulin levels at time points 0 and 30 min (when the peak insulin level is often observed) are also quantified. As shown in Figures 3E−H and S1, all four groups exhibited adequate glucose responsiveness at week 12 (Figures 3E,F and S1A) with similar levels of serum insulin (Figure S1C). However, by week 20, only mice from the PLGA(PEP) group remained glucose responsive, while mice from all three other groups showed impaired glucose tolerance (Figures 3G,H and S1B). Moreover, the average

https://dx.doi.org/10.1021/acs.molpharmaceut.0c00525
Mol. Pharmaceutics 2020, 17, 3513−3525

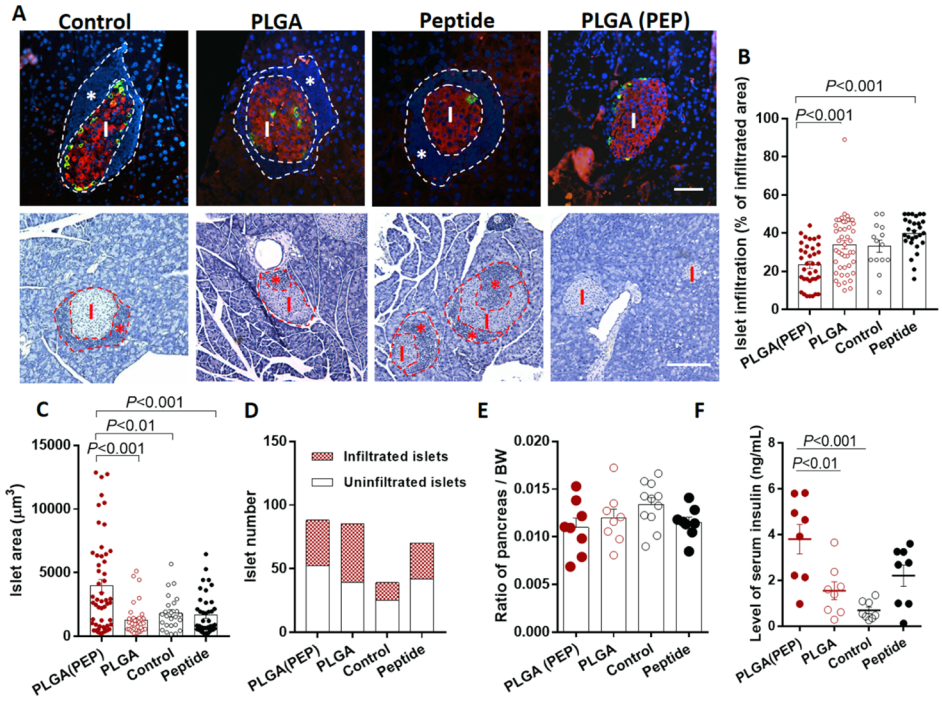

Figure 4. PLGA microparticles + $Ins2_{9-23}$ immunization ameliorated immune cell infiltration of pancreatic islets. (A) Representative images of immunofluorescence staining (upper panels) and histological staining (lower panels) of pancreatic islets from mice immunized with $Ins2_{9-23}$ (Peptide), blank PLGA microparticles (PLGA), PLGA microparticles + $Ins2_{9-23}$ (PLGA[PEP]), and PBS (Control). For immunofluorescence staining images, the insulin-secreting β-cells are shown in red, while the glucagon-producing α-cells are shown in green. Cell nuclei were stained with DAPI and shown in blue. Uninfiltrated islet areas are labeled with "I" and areas with immune cell infiltration are marked with "*". Scale bar = 100 μm. (B) Islet infiltration was quantified and expressed as the average percentage of infiltrated area over the whole islet for each islet for every treatment group. (C) Average size of islets found in each treatment group. (D) Proportion of infiltrated and uninfiltrated islets for each treatment group, n = 14−52. (E) Pancreas organ index (ratio of the weight of pancreas over body weight), n = 8−10. (F) ELISA quantification of average serum insulin levels of all treatment groups. Statistical significance was assessed using one-way ANOVA with Tukey's post hoc test, n = 7−10.

serum insulin level of mice from the control group is also significantly lower than the other three groups (Figure S1D,E), indicating deteriorated endogenous insulin secretion. Average body weights of all four treatment groups were between 25 and 30 g with no major fluctuation, as presented in Figure 3D, indicating no noticeable systemic toxicity.

As the onset of T1D is mainly caused by autoimmunity against the pancreatic islets, the morphology of islets was also examined. As shown in Figures 4A and S2, pancreatic islets were outlined by white dotted lines for fluorescence staining images and red dotted lines for histological staining images. Uninfiltrated islet areas are marked by "I" and areas that have been infiltrated by immune cells are marked with "*". Thus, it is evident that islets from the PLGA(PEP) group showed minimal immune cell infiltration. In contrast, the other three treatment groups all exhibit various degrees of moderate islet infiltration, corresponding to worsened glycemic control in these three groups. Furthermore, both fluorescence and histological staining revealed comparatively low level of immune cell infiltration in islets of PLGA(PEP) mice (23.39 ± 1.8%, n = 36; Figure 4B). A moderate degree of islet infiltration was observed from PLGA and Peptide groups (34.02 ± 2.2%, n = 46 for PLGA; 39.86 ± 1.7%, n = 28 for the Peptide group; Figure 4B). By double-labeling pancreatic sections with insulin and CD45, a lymphocyte marker, we also observed that the infiltrated immune cells within the pancreatic islets are largely of $CD45^+$ lymphocyte origin (Figure S2).

In addition, islets from the PLGA(PEP) group were also comparatively larger (Figure 4C), again demonstrative of better islet survival and, consequently, protection from the onset of diabetes. It is worth noting that despite significant T1D progression, the degree of islet infiltration from the control group appeared to be lower (Figure 4B, 33%, n = 14). The reason for this is low islet count, which corresponds to the considerably fewer number of islets left in mice from the control group at week 30 in comparison to the other three groups, despite a similar pancreas organ index among all four treatment groups (Figure 4E). This, in turn, is likely caused by the accelerated islet attrition in the control group. Indeed, it is evident from Figure 4D that mice from the control group have the lowest islet number, and as islet death is a gradual and unsynchronized process,[52] the remaining islets and their morphology can only partially represent the severity of autoimmunity against the pancreatic β-cells and islet loss. Moreover, the serum insulin level of mice treated with PLGA(PEP) was also significantly higher than the mice treated with blank PLGA and untreated controls (246 ± 42% over PLGA, P < 0.01; 549 ± 93% over Control, P < 0.001; 172 ± 29% over Peptide, P > 0.05; Figure 4F).

3.4. Effect of PLGA Microparticles + $Ins2_{9-23}$ on Thymus T-Cell Development. The excellent preventive property of PLGA microparticles + $Ins2_{9-23}$ is intriguing as although MHC II mutation has been implicated in T1D development, the MHC II molecule is in fact incapable of distinguishing between "self" and "foreign" during antigen presentation. Furthermore, as most of the internal antigens presented by MHC II are indeed autoantigens, it is the T lymphocytes that are responsible for determining the

https://dx.doi.org/10.1021/acs.molpharmaceut.0c00525
Mol. Pharmaceutics 2020, 17, 3513−3525

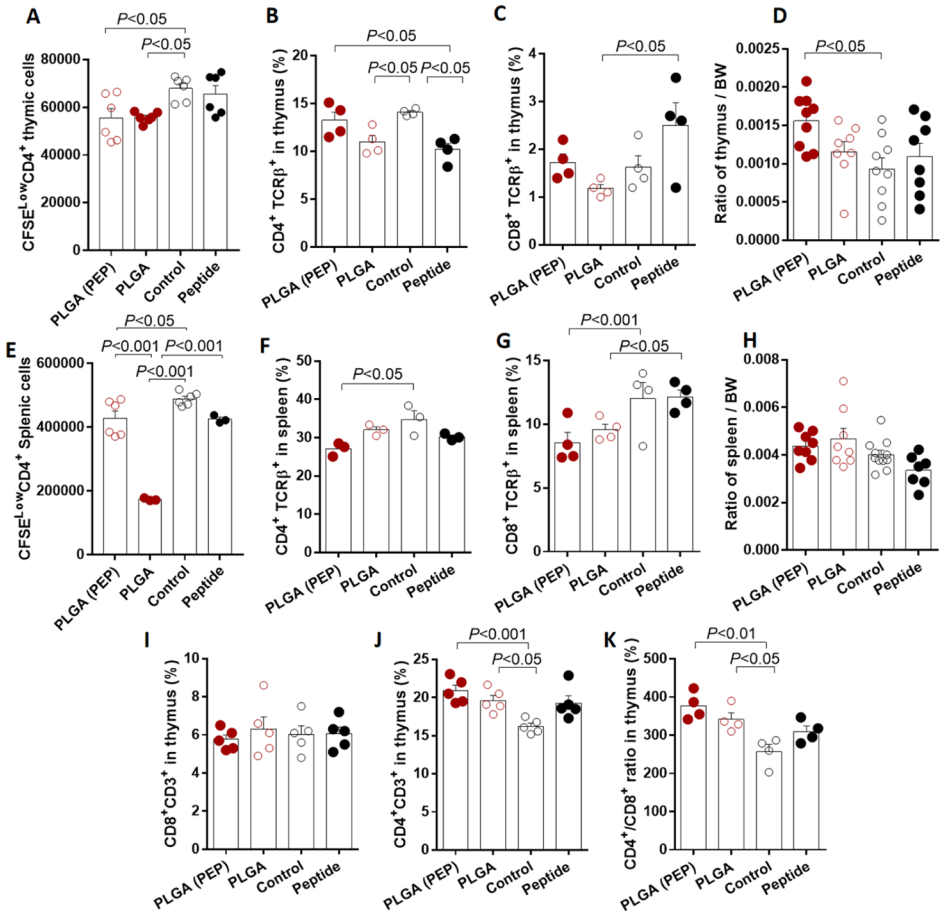

Figure 5. Effect of PLGA microparticles + $Ins2_{9-23}$ immunization on T-cell development in the thymus and spleen. (A,E) $CD4^+$ T-cell proliferation following $Ins2_{9-23}$ peptide restimulation in thymic (A) and splenic (E) lymphocytes isolated from mice immunized with $Ins2_{9-23}$ (Peptide), blank PLGA microparticles (PLGA), PLGA microparticles + $Ins2_{9-23}$ (PLGA[PEP]), and PBS (Control), n = 4−6. (B,F) Percentage of CD4+/TCRβ^+ cells in mouse thymus (B) and spleen (F) of all treatment groups, n = 4−6. (C,G) Percentage of $CD8^+$/TCRβ^+ cells in the mouse thymus (C) and spleen (G) of all treatment groups, n = 4−6. (D,H) Organ indexes of the thymus (D) and spleen (H) in mice from all treatment groups, n = 8−10. (I−K) CD3, CD4, and CD8 expression in splenic T-cells from mice of all four treatment groups, n = 4−6. Data represent mean + s.e.m. Statistical significance was assessed using one-way ANOVA with Tukey's post hoc test.

consequence of a specific antigen presented by MHC II, that is, whether to induce immune attack or immune tolerance. As a result, we have subsequently examined the potential effect of PLGA microparticles + $Ins2_{9-23}$ on T-cell development in the thymus and the spleen.

To examine the impact of PLGA(PEP) on T-cell development in thymus, we performed the antigen recall T-cell proliferation assay in T-cells obtained from mouse thymus of each treatment group at week 20. As shown in Figure 5A, thymic T-cells were extracted from all four treatment groups and labeled with CFSE, a fluorescent dye. These T-cells were then exposed to $Ins2_{9-23}$ for 3 days. The MFI of CFSE was then quantified by flow cytometry, and it is evident that T-cells of the PLGA(PEP) group showed the lowest MFI value, which correspond to the most rapid cell turnover (82 ± 6% over Control, $P < 0.05$). Surprisingly, cells extracted from mice treated with blank PLGA microparticles also showed increased proliferation in the presence of latent $Ins2_{9-23}$ stimulation (shown by the decreased CFSE MFI value, 82 ± 1% over Control, $P < 0.05$), implicating an antigen-dependent adjuvant role of the PLGA microparticles in T-cell proliferation.

However, the ultimate fate following T-cell differentiation (whether it would be $CD4^+$ or $CD8^+$) is determined by expression of the CD4 or CD8 surface marker in the presence of a costimulatory molecule, the TCRs. Only if a T-cell is double positive for both CD4 and TCR, this specific T-cell would become designated for a $CD4^+$ T-cell, and it is the same for $CD8^+$ T-cells. When we analyzed the percentage of $CD4^+$/TCRβ^+ and $CD8^+$/TCRβ^+ cell populations within the thymus by the age of week 30, we observed that there was an increased $CD4^+$/TCRβ^+ cell count in PLGA(PEP)-treated mice compared to mice immunized by $Ins2_{9-23}$ only (Figure 5B; 130 ± 8% over Peptide, $P < 0.05$). However, no significant difference was detected between the PLGA(PEP) and control groups (94 ± 6% over Control, $P = 0.8$; Figure 5B). In addition, the percentage of $CD8^+$/TCRβ^+ cells was higher in the peptide group than in the others (Figure 5C). It is still noteworthy that the PLGA(PEP) group had a higher level of $CD4^+$/TCRβ^+ cells in the thymus than the peptide-only group, which again may implicate an adjuvant property of PLGA on antigen-induced $CD4^+$ T-cell generation. Moreover, the average weight of thymus also differs, in that mice from the PLGA(PEP) group exhibit the highest value of organ index (ratio of thymus to body weight); in contrast, the thymus from the control group was rather shriveled and smaller in size (Figure 5D). In addition, we also double-labeled the thymic T-cells with $CD4^+$/$CD3^+$ or $CD8^+$/$CD3^+$ and, consistently, a significantly higher percentage of $CD4^+$/$CD3^+$ T-cells and an

https://dx.doi.org/10.1021/acs.molpharmaceut.0c00525
Mol. Pharmaceutics 2020, 17, 3513−3525

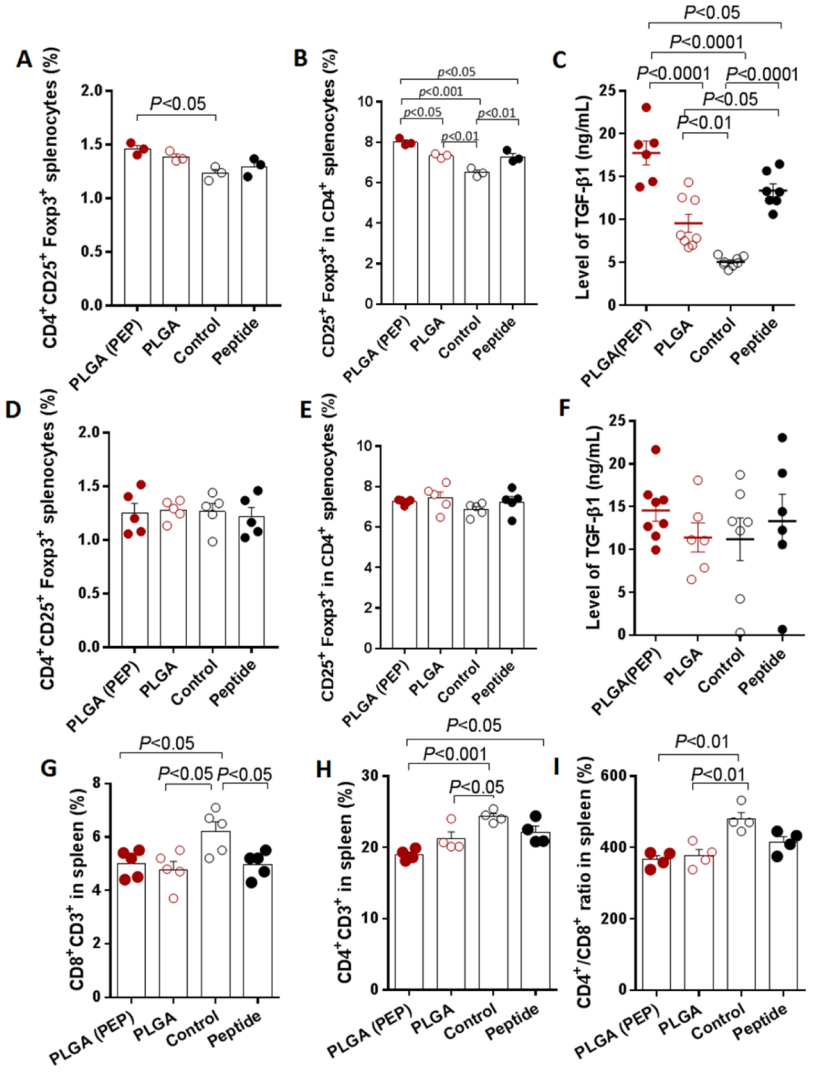

Figure 6. PLGA microparticles + $Ins2_{9-23}$ immunization-induced peripheral immune tolerance. (A,B,D,E) Percentage of $CD4^+CD25^+FOXP3^+$ Tregs in splenocytes in mice at the age of week 20 (A,B) and week 30 (D,E), n = 4−6. (C,F) Serum TGF-β1 levels in mice at the age of week 20 (C) and week 30 (F), n = 6−8. (G−I) CD3, CD4, and CD8 expression in splenic T-cells from mice of all four treatment groups, n = 4−6. Data represent mean ± s.e.m. Statistical significance was assessed using one-way ANOVA with Tukey's post hoc test.

increased ratio of $CD4^+/CD8^+$ T-cells were observed from both PLGA(PEP) and PLGA groups (Figure 5I−K).

Following T-cell differentiation, T-cells that have been activated by MHC II may undergo a process called negative selection (also known as T-cell deletion), during which they become apoptotic or inactivated. This would lead to the self-deletion of T-cells that recognize autoantigens and, thus, induce immune tolerance against these autoantigens. As mentioned before, in peripheral organs, we have observed that lymphocyte infiltration is significantly ameliorated in PLGA(PEP)-treated mice compared to the controls in the pancreas (Figures 4A and S2). It is also possible that the increase of $CD4^+$ T-cell population in the thymus reflects increased thymic Treg population, but as shown in Figure S3, we did not observe any significant differences in $FOXP3^+CD25^+CD4^+$ cells among all treatment groups.

In the spleen, the lowest percentage of $CD4^+/TCR\beta^+$ T-cells was measured from the mouse spleen of the PLGA(PEP) group (Figure 5F), while, as expected, the control group had the highest level of $CD8^+/CD3^+$ T-cells in the spleen (Figure 6G−I), corresponding to exacerbated immune attack. For the PLGA(PEP) group, the decreased percentage of splenic $CD4^+/CD3^+$ was also quantified compared to controls (Figure 6G−I in the spleen). As negative selection could occur during T-cell maturation and differentiation in the thymus before they reach the periphery and take effect, it is possible that the ameliorative impact of PLGA(PEP) on T1D progression may be partly attributable to its potential impact on thymus T-cell negative selection, which is worthy of future exploration. Interestingly, blank PLGA microparticles alone induced substantial proliferation of splenic $CD4^+$ T-cells (Figure 5E), once again emphasizing the role of PLGA microparticles in $CD4^+$ T-cell regulation.

3.5. PLGA Microparticles + $Ins2_{9-23}$-Induced Peripheral Immune Tolerance by Stimulating Splenic Treg Proliferation and Function. Regarding the peripheral immune tolerance induction, we detected a stimulatory impact of PLGA microparticles on splenic Treg augmentation and TGF-β1 release (Figure 6A−C), both of which are crucial regulators of immune tolerance. However, the stimulatory effect was lost by week 30 (Figure 6D−F), highlighting the fact

https://dx.doi.org/10.1021/acs.molpharmaceut.0c00525
Mol. Pharmaceutics 2020, 17, 3513−3525

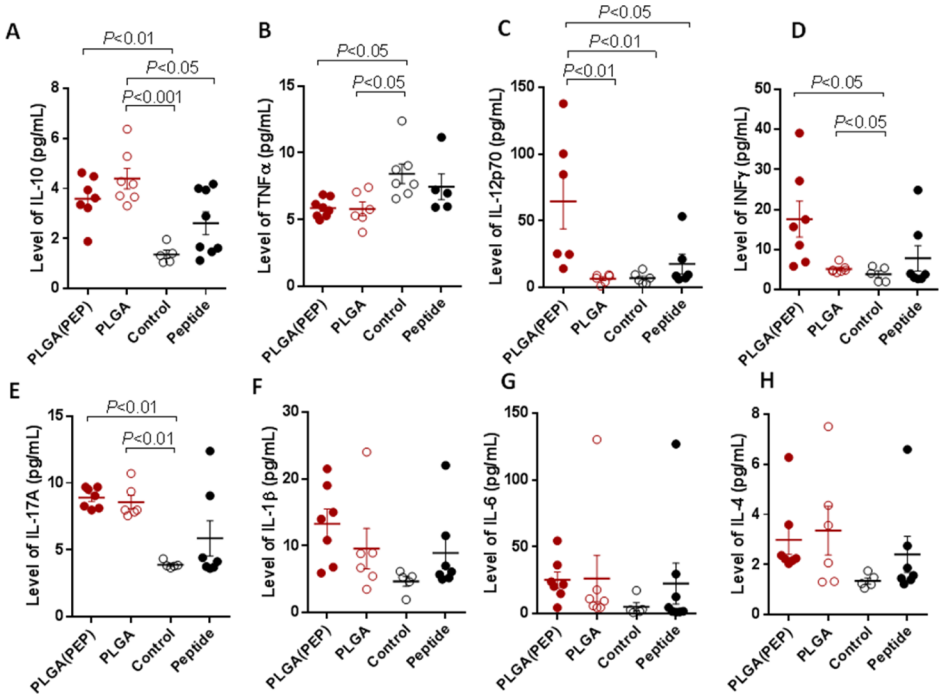

Figure 7. PLGA microparticles + $Ins2_{9-23}$-induced peripheral immune responses by regulating systemic cytokine production. Multiplex ELISA quantification of serum cytokine IL-10 (A), TNF-α (B), IL-12p70 (C), INF-γ (D), IL-17A (E), IL-1β (F), IL-6 (G), and IL-4 (H) levels of all treatment groups. Data represent mean ± s.e.m, n = 6−9. Statistical significance was assessed using one-way ANOVA with Tukey's post hoc test.

that timing is critical for the successful induction of immune tolerance and T1D prevention.

This was confirmed by the results obtained by multiplex serum cytokine ELISA (Figure 7), in which significantly increased levels of IL-10, a regulatory cytokine known to be crucial in autoimmune and allergic responses by promoting phagocytic uptake and Th2 responses, were detected in both PLGA(PEP) and PLGA groups (Figure 7A, 262 ± 25 and 321 ± 30% for PLGA[PEP] and PLGA, respectively, over Control, $P < 0.01$). Similarly, the serum concentration of TNF-α was lower in animals of the PLGA(PEP) and PLGA groups, as compared to controls (Figure 7B; 70 ± 3 and 69 ± 6% for PLGA[PEP] and PLGA respectively, over Control, $P < 0.05$).

Counterintuitively, perhaps, we also observed increased serum levels of IL-12p70 (901 ± 287% over Control, $P < 0.01$) and INF-γ (452 ± 115% over Control, $P < 0.01$) in the PLGA(PEP) group in comparison to controls, both of which are regarded as proinflammatory, and stimulate antigen presentation from DCs and macrophages (Figure 7C,D). In addition, both PLGA(PEP) and PLGA groups showed elevated serum levels of IL-17A, a cytokine secreted by Th17 cells, which has been reported to respond to INF-γ (Th1) and TGF-β (Tregs) (Figure 7E). No significant differences were detectable in the serum levels of IL-1β (Figure 7F), IL-6 (Figure 7G), or IL-4 (Figure 7H) among all four treatment groups.

Importantly, it is worth noting that PLGA microparticles per se induced substantial elevation of serum IL-10 (Figure 7A), TGF-β1 (Figure 6C), and, arguably, IL-17A (Figure 7E) levels, highlighting a tolerance-inducing property of PLGA microparticles in the periphery. Simultaneously, PLGA microparticles alone only weakly stimulated serum INF-γ (as well as IL-17A), implicating a comparatively weak (partly due to the lack of antigen in the PLGA microparticles-only [PLGA] group) but stimulatory effect on antigen presentation, both of which are responsible for the moderate preventive impact of blank PLGA microparticles on T1D onset. This is further supported by studies reporting that proinflammatory adjuvants, such as GM-CSF, a chemoattractant able to activate antigen-presenting cells while recruiting circulating lymphocytes and neutrophils, and CpG,[53] a Toll-like receptor 9 agonist[54] that stimulates proinflammatory effects such as interferon gamma (IFN-γ) production and nuclear factor kappa B (NF-κB) signaling, have all been implicated in inducing immune responses in autoimmune diseases and allergy.[38] Furthermore, as discussed earlier, one of the reasons that NOD mice develop T1D is that they were born with a defect in DC maturation and, therefore, antigen presentation (which is rather similar to T1D patients with MHC II mutation and dysfunction);[14] this inadequate antigen presentation would lead to inefficient T-cell recognition of autoantigens and impaired generation of $CD4^+$/$TCR\beta^+$ T-cells which, in turn, renders the T-cell negative selection process ineffective. Furthermore, it has been recently reported that IL-12 exposure-elicited IFN-γ could prevent the onset of T1D in NOD mice by inhibiting Th-17 cells and their associated proinflammatory cytokine secretion,[55,56] while it was also reported that IL-12 (with IL-2 and IL-15) may also stimulate the activity of natural killer (NK) cells from the peripheral blood of T1D children and IL-10 synthesis, thereby inhibiting autoimmune reaction.[57] In addition, the pathogenic role of Th-17 cells as well as of Il-17 may also be responsible for diabetes development,[58−60] indicating, as expected, more complicated signaling crosstalk and regulation of different immune mediators in autoimmune reactions.

As a result, the autoantigen, in this case, insulin, would be treated as foreign and attacked by "untrained" T-cells. PLGA microparticle delivery of $Ins2_{9-23}$ and the $Ins2_{9-23}$ peptide per se, to a certain extent, was able to compensate for the insufficient autoantigen presentation by enhancing the DC function and MHC II presentation and "re-introducing" the

https://dx.doi.org/10.1021/acs.molpharmaceut.0c00525
Mol. Pharmaceutics 2020, 17, 3513−3525

self-antigen to T-cells for negative selection and achieve "re-education" of the immune system. For PLGA microparticles per se, the observed immune tolerance induction, albeit not much effective without an autoantigen, is likely to be primarily mediated by activating the peripheral immune tolerance mechanism.

4. CONCLUSIONS

In summary, we report here a possible adjuvant property of PLGA microparticles for immune tolerance induction against T1D progression. Considering that the immune adjuvant is crucial to eliciting desirable responses for the modulation of adaptive immunity and that T1D is one common form of autoimmune diseases, PLGA microparticles could potentially be useful for the treatment of other autoimmune diseases, such as the devastating multiple sclerosis or lupus erythematosus. Furthermore, with both PLGA and insulin peptide fragment being proved to be relatively safe in humans, data presented in this study would also have a positive implication on the development of T1D prevention approaches in humans.

■ ASSOCIATED CONTENT

Supporting Information

The Supporting Information is available free of charge at https://pubs.acs.org/doi/10.1021/acs.molpharmaceut.0c00525.

Quantification of the plasma glucose level and serum insulin level during the first 30 min of the IPGTT test; pancreatic islet infiltrate of female NOD mice, which is mainly composed of $CD45^+$ lymphocytes; and measurement of Treg proportion in the thymus (PDF)

■ AUTHOR INFORMATION

Corresponding Author

Chen Li − *Tianjin Key Laboratory of Biomedical Materials, Biomedical Barriers Research Centre, Institute of Biomedical Engineering, Chinese Academy of Medical Sciences & Peking Union Medical College, Tianjin 300192, China;* orcid.org/0000-0002-8444-8739; Email: cli@bme.pumc.edu.cn

Authors

Mohan Liu − *Tianjin Key Laboratory of Biomedical Materials, Biomedical Barriers Research Centre, Institute of Biomedical Engineering, Chinese Academy of Medical Sciences & Peking Union Medical College, Tianjin 300192, China*

Dandan Feng − *Tianjin Key Laboratory of Biomedical Materials, Biomedical Barriers Research Centre, Institute of Biomedical Engineering, Chinese Academy of Medical Sciences & Peking Union Medical College, Tianjin 300192, China*

Xiaoyu Liang − *Tianjin Key Laboratory of Biomedical Materials, Biomedical Barriers Research Centre, Institute of Biomedical Engineering, Chinese Academy of Medical Sciences & Peking Union Medical College, Tianjin 300192, China*

Min Li − *Tianjin Key Laboratory of Biomedical Materials, Biomedical Barriers Research Centre, Institute of Biomedical Engineering, Chinese Academy of Medical Sciences & Peking Union Medical College, Tianjin 300192, China*

Jing Yang − *Tianjin Key Laboratory of Biomedical Materials, Biomedical Barriers Research Centre, Institute of Biomedical Engineering, Chinese Academy of Medical Sciences & Peking Union Medical College, Tianjin 300192, China;* orcid.org/0000-0003-3848-5958

Hai Wang − *Tianjin Key Laboratory of Biomedical Materials, Biomedical Barriers Research Centre, Institute of Biomedical Engineering, Chinese Academy of Medical Sciences & Peking Union Medical College, Tianjin 300192, China*

Liyun Pang − *Tianjin Key Laboratory of Biomedical Materials, Biomedical Barriers Research Centre, Institute of Biomedical Engineering, Chinese Academy of Medical Sciences & Peking Union Medical College, Tianjin 300192, China*

Zhimin Zhou − *Tianjin Key Laboratory of Biomedical Materials, Biomedical Barriers Research Centre, Institute of Biomedical Engineering, Chinese Academy of Medical Sciences & Peking Union Medical College, Tianjin 300192, China*

Zhimou Yang − *Key Laboratory of Bioactive Materials, Ministry of Education, College of Life Sciences, State Key Laboratory of Medicinal Chemical Biology, Collaborative Innovation Centre of Chemical Science and Engineering, and National Institute of Functional Materials, Nankai University, Tianjin 300071, China;* orcid.org/0000-0003-2967-6920

Deling Kong − *Key Laboratory of Bioactive Materials, Ministry of Education, College of Life Sciences, State Key Laboratory of Medicinal Chemical Biology, Collaborative Innovation Centre of Chemical Science and Engineering, and National Institute of Functional Materials, Nankai University, Tianjin 300071, China;* orcid.org/0000-0002-5520-0769

Complete contact information is available at: https://pubs.acs.org/10.1021/acs.molpharmaceut.0c00525

Author Contributions

M.L. and D.F. contributed equally to this work. C.L. conceived and designed the experiments. M.L.D.F., X.L., and M.L. conducted the experiments. J.Y., H.W., L.P., and Z.Z. contributed to data analysis and interpretation. C.L. drafted the manuscript. D.K. and Z.Y. critically examined the data and manuscript. All authors have read and approved the final manuscript.

Notes

The authors declare no competing financial interest.

Raw data required to reproduce these findings are available upon request. The processed data required to reproduce these findings are available to download upon request.

■ ACKNOWLEDGMENTS

This work was financially supported by the National Natural Science Foundation of China (no. 31770968), Specific Program for High-Tech Leader & Team of Tianjin Government, and Tianjin Innovation & Promotion Plan Key Innovation Team of Immunoreactive Biomaterials. C.L. was funded by the Tianjin Research Program for Distinguished Young Scholar (18JCJQJC48100), the Tianjin Association for Science & Technology Youth Talent Promotion Project, and the Non-profit Central Research Institute Fund of the Chinese Academy of Medical Sciences (no. 2018RC350018).

■ REFERENCES

(1) Garyu, J. W.; Meffre, E.; Cotsapas, C.; Herold, K. C. *J. Autoimmun.* **2016**, *71*, 1−9.

(2) Imperatore, G.; Boyle, J. P.; Thompson, T. J.; Case, D.; Dabelea, D.; Hamman, R. F.; Lawrence, J. M.; Liese, A. D.; Liu, L. L.; Mayer-Davis, E. J.; Rodriguez, B. L.; Standiford, D. *Diabetes Care* **2012**, *35*, 2515−2520.

(3) DiMeglio, L. A.; Evans-Molina, C.; Oram, R. A. *Lancet* **2018**, *391*, 2449−2462.

(4) Bluestone, J. A.; Herold, K.; Eisenbarth, G. *Nature* **2010**, *464*, 1293−1300.
(5) Miller, K. M.; Foster, N. C.; Beck, R. W.; Bergenstal, R. M.; DuBose, S. N.; DiMeglio, L. A.; Maahs, D. M.; Tamborlane, W. V. *Diabetes Care* **2015**, *38*, 971−978.
(6) Herold, K. C.; Hagopian, W.; Auger, J. A.; Poumian-Ruiz, E.; Taylor, L.; Donaldson, D.; Gitelman, S. E.; Harlan, D. M.; Xu, D.; Zivin, R. A.; Bluestone, J. A. *N. Engl. J. Med.* **2002**, *346*, 1692−1698.
(7) Keymeulen, B.; Vandemeulebroucke, E.; Ziegler, A. G.; Mathieu, C.; Kaufman, L.; Hale, G.; Gorus, F.; Goldman, M.; Walter, M.; Candon, S.; Schandene, L.; Crenier, L.; De Block, C.; Seigneurin, J.-M.; De Pauw, P.; Pierard, D.; Weets, I.; Rebello, P.; Bird, P.; Berrie, E.; Frewin, M.; Waldmann, H.; Bach, J.-F.; Pipeleers, D.; Chatenoud, L. *N. Engl. J. Med.* **2005**, *352*, 2598−2608.
(8) Rigby, M. R.; DiMeglio, L. A.; Rendell, M. S.; Felner, E. I.; Dostou, J. M.; Gitelman, S. E.; Patel, C. M.; Griffin, K. J.; Tsalikian, E.; Gottlieb, P. A.; Greenbaum, C. J.; Sherry, N. A.; Moore, W. V.; Monzavi, R.; Willi, S. M.; Raskin, P.; Moran, A.; Russell, W. E.; Pinckney, A.; Keyes-Elstein, L.; Howell, M.; Aggarwal, S.; Lim, N.; Phippard, D.; Nepom, G. T.; McNamara, J.; Ehlers, M. R. *Lancet Diabetes Endocrinol.* **2013**, *1*, 284−294.
(9) Miller, S. D.; Turley, D. M.; Podojil, J. R. *Nat. Rev. Immunol.* **2007**, *7*, 665−677.
(10) Serra, P.; Santamaria, P. *Nat. Biotechnol.* **2019**, *37*, 238−251.
(11) Burks, A. W.; Jones, S. M.; Wood, R. A.; Fleischer, D. M.; Sicherer, S. H.; Lindblad, R. W.; Stablein, D.; Henning, A. K.; Vickery, B. P.; Liu, A. H.; Scurlock, A. M.; Shreffler, W. G.; Plaut, M.; Sampson, H. A. *N. Engl. J. Med.* **2012**, *367*, 233−243.
(12) Pearson, R. M.; Podojil, J. R.; Shea, L. D.; King, N. J. C.; Miller, S. D.; Getts, D. R. *Nanomedicine* **2019**, *18*, 282−291.
(13) Alhadj Ali, M.; Liu, Y.-F.; Arif, S.; Tatovic, D.; Shariff, H.; Gibson, V. B.; Yusuf, N.; Baptista, R.; Eichmann, M.; Petrov, N.; Heck, S.; Yang, J. H. M.; Tree, T. I. M.; Pujol-Autonell, I.; Yeo, L.; Baumard, L. R.; Stenson, R.; Howell, A.; Clark, A.; Boult, Z.; Powrie, J.; Adams, L.; Wong, F. S.; Luzio, S.; Dunseath, G.; Green, K.; O'Keefe, A.; Bayly, G.; Thorogood, N.; Andrews, R.; Leech, N.; Joseph, F.; Nair, S.; Seal, S.; Cheung, H.; Beam, C.; Hills, R.; Peakman, M.; Dayan, C. M. *Sci. Transl. Med.* **2017**, *9*, eaaf7779.
(14) Stewart, J. M.; Keselowsky, B. G. *Adv. Drug Delivery Rev.* **2017**, *114*, 161−174.
(15) Cabello-Olmo, M.; Araña, M.; Radichev, I.; Smith, P.; Huarte, E.; Barajas, M. *Int. J. Mol. Sci.* **2019**, *20*, 4789.
(16) Beam, C. A.; MacCallum, C.; MacCallum, C.; Herold, K. C.; Palmer, D. K.; Ludvigsson, J. *Diabetologia* **2017**, *60*, 43−49.
(17) Wherrett, D. K.; Bundy, B.; Becker, D. J.; DiMeglio, L. A.; Gitelman, S. E.; Goland, R.; Gottlieb, P. A.; Greenbaum, C. J.; Herold, K. C.; Marks, J. B.; Monzavi, R.; Moran, A.; Orban, T.; Palmer, J. P.; Raskin, P.; Rodriguez, H.; Schatz, D.; Wilson, D. M.; Krischer, J. P.; Skyler, J. S. *Lancet* **2011**, *378*, 319−327.
(18) Shi, G.-N.; Zhang, C.-N.; Xu, R.; Niu, J.-F.; Song, H.-J.; Zhang, X.-Y.; Wang, W.-W.; Wang, Y.-M.; Li, C.; Wei, X.-Q.; Kong, D.-L. *Biomaterials* **2017**, *113*, 191−202.
(19) Liang, X.; Duan, J.; Li, X.; Zhu, X.; Chen, Y.; Wang, X.; Sun, H.; Kong, D.; Li, C.; Yang, J. *Nanoscale* **2018**, *10*, 9489−9503.
(20) Shields, C. W.; Wang, L. L.-W.; Evans, M. A.; Mitragotri, S. *Adv. Mater.* **2020**, *32*, 1901633.
(21) Min, Y.; Roche, K. C.; Tian, S.; Eblan, M. J.; McKinnon, K. P.; Caster, J. M.; Chai, S.; Herring, L. E.; Zhang, L.; Zhang, T.; DeSimone, J. M.; Tepper, J. E.; Vincent, B. G.; Serody, J. S.; Wang, A. Z. *Nat. Nanotechnol.* **2017**, *12*, 877−882.
(22) Kishimoto, T. K.; Ferrari, J. D.; LaMothe, R. A.; Kolte, P. N.; Griset, A. P.; O'Neil, C.; Chan, V.; Browning, E.; Chalishazar, A.; Kuhlman, W.; Fu, F.-n.; Viseux, N.; Altreuter, D. H.; Johnston, L.; Maldonado, R. A. *Nat. Nanotechnol.* **2016**, *11*, 890−899.
(23) Singha, S.; Shao, K.; Ellestad, K. K.; Yang, Y.; Santamaria, P. *ACS Nano* **2018**, *12*, 10621−10635.
(24) Lu, T.; Hu, F.; Yue, H.; Yang, T.; Ma, G. *J. Controlled Release* **2020**, *321*, 576−588.
(25) Kwiatkowski, A. J.; Stewart, J. M.; Cho, J. J.; Avram, D.; Keselowsky, B. G. *Adv. Healthcare Mater.* **2020**, *9*, e2000164.
(26) Carballido, J. M.; Santamaria, P. *J. Exp. Med.* **2019**, *216*, 247−250.
(27) Yeste, A.; Nadeau, M.; Burns, E. J.; Weiner, H. L.; Quintana, F. J. *Proc. Natl. Acad. Sci. U.S.A.* **2012**, *109*, 11270−11275.
(28) Zhang, T.; Li, M.; Wang, X.; Zhou, Z.; Yuan, W.; Ma, J. *Chem. Commun.* **2018**, *54*, 11356−11359.
(29) Clemente-Casares, X.; Blanco, J.; Ambalavanan, P.; Yamanouchi, J.; Singha, S.; Fandos, C.; Tsai, S.; Wang, J.; Garabatos, N.; Izquierdo, C.; Agrawal, S.; Keough, M. B.; Yong, V. W.; James, E.; Moore, A.; Yang, Y.; Stratmann, T.; Serra, P.; Santamaria, P. *Nature* **2016**, *530*, 434−440.
(30) Li, Q.; Zhang, Y.; Li, J.; Wang, H.; Lu, H.; Fan, H.; Zheng, G. *Mater. Express* **2019**, *9*, 962−969.
(31) Martins, C.; Sousa, F.; Araujo, F.; Sarmento, B. *Adv. Healthcare Mater.* **2018**, *7*, 1701035.
(32) Du, B.; Wang, J.; Zhou, Z.; Tang, H.; Li, X.; Liu, Y.; Zhang, Q. *Chem. Commun.* **2014**, *50*, 4423−4426.
(33) Li, R.; Li, X.; Liu, L.; Zhou, Z.; Tang, H.; Zhang, Q. *Macromol. Rapid Commun.* **2010**, *31*, 1981−1986.
(34) Qiao, F.; Zhang, J.; Wang, J.; Du, B.; Huang, X.; Pang, L.; Zhou, Z. *Colloids Surf., B* **2017**, *158*, 112−118.
(35) Khan, F.; Aldhahri, M.; Hussain, M. A.; Gauthaman, K.; Memic, A.; Abuzenadah, A.; Kumosani, T.; Barbour, E.; Alothmany, N. S.; Aldhaheri, R. W. *J. Biomed. Nanotechnol.* **2018**, *14*, 553−563.
(36) Allen, R. P.; Bolandparvaz, A.; Ma, J. A.; Manickam, V. A.; Lewis, J. S. *ACS Biomater. Sci. Eng.* **2018**, *4*, 900−918.
(37) Verbeke, C. S.; Gordo, S.; Schubert, D. A.; Lewin, S. A.; Desai, R. M.; Dobbins, J.; Wucherpfennig, K. W.; Mooney, D. J. *Adv. Healthcare Mater.* **2017**, *6*, 1600773.
(38) Yoon, Y. M.; Lewis, J. S.; Carstens, M. R.; Campbell-Thompson, M.; Wasserfall, C. H.; Atkinson, M. A.; Keselowsky, B. G. *Sci. Rep.* **2015**, *5*, 13155.
(39) Prasad, S.; Neef, T.; Xu, D.; Podojil, J. R.; Getts, D. R.; Shea, L. D.; Miller, S. D. *J. Autoimmun.* **2018**, *89*, 112−124.
(40) Lewis, J. S.; Stewart, J. M.; Marshall, G. P.; Carstens, M. R.; Zhang, Y.; Dolgova, N. V.; Xia, C.; Brusko, T. M.; Wasserfall, C. H.; Clare-Salzler, M. J.; Atkinson, M. A.; Keselowsky, B. G. *ACS Biomater. Sci. Eng.* **2019**, *5*, 2631−2646.
(41) Zhang, W.; Wang, L.; Yang, T.; Liu, Y.; Chen, X.; Liu, Q.; Jia, J.; Ma, G. *Pharm. Res.* **2015**, *32*, 2837−2850.
(42) Halbout, P.; Briand, J.-P.; Bécourt, C.; Muller, S.; Boitard, C. *J. Immunol.* **2002**, *169*, 2436−2443.
(43) Jarchum, I.; DiLorenzo, T. P. *J. Immunol.* **2010**, *184*, 658−665.
(44) Mao, D.; Zhu, M.; Zhang, X.; Ma, R.; Yang, X.; Ke, T.; Wang, L.; Li, Z.; Kong, D.; Li, C. *Acta Biomater.* **2017**, *59*, 210−220.
(45) Gao, S.; Zhang, X.; Qin, Y.; Xu, S.; Zhang, J.; Wang, Z.; Wang, W.; Kong, D.; Li, C. *Clin. Sci.* **2016**, *130*, 1901−1911.
(46) Zhou, Z.; Xu, J.; Liu, X.; Li, X.; Li, S.; Yang, K.; Wang, X.; Liu, M.; Zhang, Q. *Polymer* **2009**, *50*, 3841−3850.
(47) Maldonado, R. A.; LaMothe, R. A.; Ferrari, J. D.; Zhang, A.-H.; Rossi, R. J.; Kolte, P. N.; Griset, A. P.; O'Neil, C.; Altreuter, D. H.; Browning, E.; Johnston, L.; Farokhzad, O. C.; Langer, R.; Scott, D. W.; von Andrian, U. H.; Kishimoto, T. K. *Proc. Natl. Acad. Sci. U.S.A.* **2015**, *112*, E156−E165.
(48) Liang, X.; Li, X.; Duan, J.; Chen, Y.; Wang, X.; Pang, L.; Kong, D.; Song, B.; Li, C.; Yang, J. *Mol. Pharmaceutics* **2018**, *15*, 508−518.
(49) Steenblock, E. R.; Fahmy, T. M. *Mol. Ther.* **2008**, *16*, 765−772.
(50) Wang, Y.; Sosinowski, T.; Novikov, A.; Crawford, F.; White, J.; Jin, N.; Liu, Z.; Zou, J.; Neau, D.; Davidson, H. W.; Nakayama, M.; Kwok, W. W.; Gapin, L.; Marrack, P.; Kappler, J. W.; Dai, S. *Sci. Immunol.* **2019**, *4*, eaav7517.
(51) Pearson, J. A.; Wong, F. S.; Wen, L. *J. Autoimmun.* **2016**, *66*, 76−88.
(52) Morgan, N. G.; Richardson, S. J. *Diabetologia* **2018**, *61*, 2499−2506.
(53) Yang, X.; Lai, C.; Liu, A.; Hou, X.; Tang, Z.; Mo, F.; Yin, S.; Lu, X. *J. Biomed. Nanotechnol.* **2019**, *15*, 1018−1032.

https://dx.doi.org/10.1021/acs.molpharmaceut.0c00525
Mol. Pharmaceutics 2020, 17, 3513−3525

(54) Zhou, Z.; Lin, H.; Li, C.; Wu, Z. *Chin. Chem. Lett.* **2018**, *29*, 19−26.
(55) Zirnheld, A. L.; Villard, M.; Harrison, A. M.; Kosiewicz, M. M.; Alard, P. *J. Leukocyte Biol.* **2019**, *106*, 1349−1358.
(56) Zhang, J.; Huang, Z.; Sun, R.; Tian, Z.; Wei, H. *J. Autoimmun.* **2012**, *38*, 20−28.
(57) Chrul, S.; Polakowska, E.; Mycko, M.; Fendler, W.; Zwiech, R.; Szadkowska, A. *Pediatr. Endocrinol., Diabetes Metab.* **2013**, *19*, 91−95.
(58) Fabbri, M.; Frixou, M.; Degano, M.; Fousteri, G. *Diabetes* **2019**, *68*, 258−265.
(59) Livanos, A. E.; Greiner, T. U.; Vangay, P.; Pathmasiri, W.; Stewart, D.; McRitchie, S.; Li, H.; Chung, J.; Sohn, J.; Kim, S.; Gao, Z.; Barber, C.; Kim, J.; Ng, S.; Rogers, A. B.; Sumner, S.; Zhang, X. S.; Cadwell, K.; Knights, D.; Alekseyenko, A.; Bäckhed, F.; Blaser, M. J. *Nat. Microbiol.* **2016**, *1*, 16140.
(60) Zheng, Z.; Zheng, F. *Mol. Immunol.* **2019**, *105*, 16−31.

https://dx.doi.org/10.1021/acs.molpharmaceut.0c00525
Mol. Pharmaceutics 2020, 17, 3513−3525